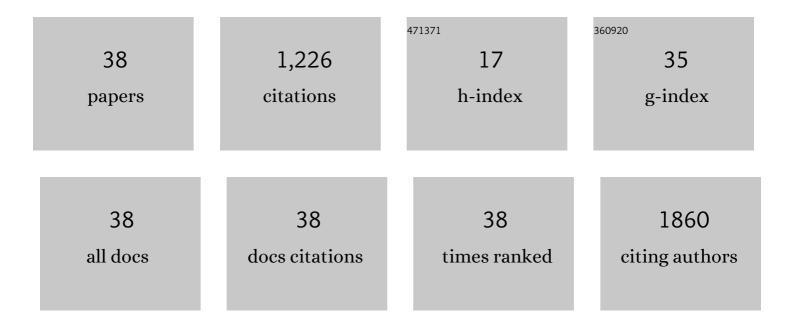
Xiaolei Guo

List of Publications by Year in descending order

Source: https://exaly.com/author-pdf/6259568/publications.pdf Version: 2024-02-01



XIAOLEL CUO

#	Article	IF	CITATIONS
1	Electrical Contact Resistance in REBCO Stacks and Cables With Modified Surfaces. IEEE Transactions on Applied Superconductivity, 2022, 32, 1-6.	1.1	4
2	Long-term interactive corrosion between International Simple Glass and stainless steel. Npj Materials Degradation, 2022, 6, .	2.6	0
3	Enhanced crevice corrosion of stainless steel 316 by degradation of Cr-containing hollandite crevice former. Corrosion Science, 2022, 205, 110462.	3.0	2
4	Electrochemical metrics for corrosion resistant alloys. Scientific Data, 2021, 8, 58.	2.4	46
5	Recent Advances in Corrosion Science Applicable To Disposal of High-Level Nuclear Waste. Chemical Reviews, 2021, 121, 12327-12383.	23.0	52
6	Corrosion inhibition of AA2024-T3 by a coating containing dual-pH sensitive, corrosion inhibitor loaded microspheres. Corrosion Science, 2021, 192, 109835.	3.0	16
7	Activation energy of metal dissolution in local pit environments. Corrosion Science, 2021, 193, 109901.	3.0	8
8	Smart coating with dual-pH sensitive, inhibitor-loaded nanofibers for corrosion protection. Npj Materials Degradation, 2021, 5, .	2.6	6
9	Reply to: How much does corrosion of nuclear waste matrices matter. Nature Materials, 2020, 19, 962-963.	13.3	7
10	Corrosion interactions between stainless steel and lead vanado-iodoapatite nuclear waste form part I. Npj Materials Degradation, 2020, 4, .	2.6	8
11	Corrosion interactions between stainless steel and lead vanado-iodoapatite nuclear waste form part II. Npj Materials Degradation, 2020, 4, .	2.6	7
12	Nanoscale TiO2 coating improves water stability of Cs2SnCl6. MRS Communications, 2020, 10, 687-694.	0.8	1
13	Degradation mechanism of lead-vanado-iodoapatite in NaCl solution. Corrosion Science, 2020, 172, 108720.	3.0	3
14	Effects of Graphene-Based Fillers on Cathodic Delamination and Abrasion Resistance of Cataphoretic Organic Coatings. Coatings, 2020, 10, 602.	1.2	18
15	Insights into the mechanisms controlling the residual corrosion rate of borosilicate glasses. Npj Materials Degradation, 2020, 4, .	2.6	26
16	Review of corrosion interactions between different materials relevant to disposal of high-level nuclear waste. Npj Materials Degradation, 2020, 4, .	2.6	20
17	Epsilon metal: A waste form for noble metals from used nuclear fuel. Journal of Nuclear Materials, 2020, 532, 152040.	1.3	3
18	Self-accelerated corrosion of nuclear waste forms at material interfaces. Nature Materials, 2020, 19, 310-316.	13.3	61

Xiaolei Guo

#	Article	IF	CITATIONS
19	Near-field corrosion interactions between glass and corrosion resistant alloys. Npj Materials Degradation, 2020, 4, .	2.6	15
20	Corrosion inhibition of AA2024-T3 by smart polyelectrolyte coacervates responsive to both acidic and alkaline environments. Progress in Organic Coatings, 2020, 146, 105719.	1.9	6
21	(Invited) Surface Analysis of Corrosion Products Built up at Interfaces of Different Nuclear Waste Forms in Near-Field Environment. ECS Meeting Abstracts, 2020, MA2020-02, 1282-1282.	0.0	0
22	Corrosion Inhibition of AA2024-T3 By Smart Polyelectrolyte Coacervates Responsive to Both Acidic and Alkaline Environments. ECS Meeting Abstracts, 2020, MA2020-02, 1346-1346.	0.0	0
23	A Novel Organic Conversion Coating based on N-Benzoyl-N-Phenylhydroxylamine Chemistry for the Corrosion Protection of AA2024-T3. Electrochimica Acta, 2017, 246, 197-207.	2.6	15
24	Administration of cells with thermosensitive hydrogel enhances the functional recovery in ischemic rat heart. Journal of Tissue Engineering, 2016, 7, 204173141664667.	2.3	13
25	Entrapped Molybdate in Phytate Film and the Corresponding Anodic Corrosion Inhibition on AA2024-T3. Journal of the Electrochemical Society, 2016, 163, C260-C268.	1.3	10
26	Encapsulation of NaVO3 as Corrosion Inhibitor into Microparticles and its Active Corrosion Protection for AA2024 Based Upon Inhibitor Control Release. Corrosion, 2015, 71, 1411-1413.	0.5	7
27	Cardiac differentiation of cardiosphere-derived cells in scaffolds mimicking morphology of the cardiac extracellular matrix. Acta Biomaterialia, 2014, 10, 3449-3462.	4.1	45
28	Electrospun Acetalated Dextran Scaffolds for Temporal Release of Therapeutics. Langmuir, 2013, 29, 7957-7965.	1.6	29
29	Periostin modulates myofibroblast differentiation during full-thickness cutaneous wound repair. Journal of Cell Science, 2012, 125, 121-132.	1.2	123
30	Creating 3D Angiogenic Growth Factor Gradients in Fibrous Constructs to Guide Fast Angiogenesis. Biomacromolecules, 2012, 13, 3262-3271.	2.6	44
31	High-efficiency matrix modulus-induced cardiac differentiation of human mesenchymal stem cells inside a thermosensitive hydrogel. Acta Biomaterialia, 2012, 8, 3586-3595.	4.1	87
32	A Thermosensitive Hydrogel Capable of Releasing bFGF for Enhanced Differentiation of Mesenchymal Stem Cell into Cardiomyocyte-like Cells under Ischemic Conditions. Biomacromolecules, 2012, 13, 1956-1964.	2.6	35
33	An oxygen release system to augment cardiac progenitor cell survival and differentiation under hypoxic condition. Biomaterials, 2012, 33, 5914-5923.	5.7	130
34	Differentiation of cardiosphere-derived cells into a mature cardiac lineage using biodegradable poly(N-isopropylacrylamide) hydrogels. Biomaterials, 2011, 32, 3220-3232.	5.7	92
35	The stimulation of the cardiac differentiation of mesenchymal stem cells in tissue constructs that mimic myocardium structure and biomechanics. Biomaterials, 2011, 32, 5568-5580.	5.7	119
36	Preparation and characterization of thermosensitive organic–inorganic hybrid microgels with functional Fe3O4 nanoparticles as crosslinker. Polymer, 2011, 52, 172-179.	1.8	70

#	Article	IF	CITATIONS
37	Preparation and functional properties of blend films of gliadins and chitosan. Carbohydrate Polymers, 2010, 81, 484-490.	5.1	42
38	PNIPAm-PEO-PPO-PEO-PNIPAm Pentablock Terpolymer: Synthesis and Chain Behavior in Aqueous Solution. Macromolecules, 2010, 43, 7312-7320.	2.2	56